Proceedings of the 9th International Conference on Cyclotrons and their Applications
September 1981, Caen, France

IPCR SEPARATED SECTOR CYCLOTRON WITH K=540

H. Kamitsubo

The Institute of Physical and Chemical Research, Wako-shi, Saitama, Japan.

Abstract.- Present status of the IPCR separated sector cyclotron project is described. The cyclotron has K number of 540 and is designed to accelerate not only heavy ions but also protons, deuterons, ^{3}He and α particles to energies higher than 100 MeV/u. Details of the project are presented.

1. Introduction.- The accelerator complex composed of a separated sector cyclotron (SSC) and two injectors is planned to be the principal facility of the accelerator science research project at the Institute of Physical and Chemical Research (IPCR)[1]. The first stage of the project was to construct the injector linac. The variable frequency heavy ion linac was completed recently. Details of the linac were reported elsewhere[2] and only a brief description of it will be given in section 3.

The second stage of the project was accepted by the government and construction of the SSC was started last year. According to our tentative schedule, the SSC will be completed in 1986 and an AVF cyclotron will be installed without interruption as the second injector.

The accelerator science research project is aimed to develop accelerator-assisted studies in the various research fields such as nuclear physics, atomic and solid state physics, nuclear and radiation chemistry, radiation biology and material engineering. Accordingly the accelerator complex should be able to accelerate not only light ions but also very heavy ions in the energy range as wide as possible. It is also required to provide a beam of good quality and of enough intensity.

The design goal of the performance of the SSC was set as follows: Maximum energies of the light heavy ions should be higher than 100 MeV/u and those of very heavy ions as high as possible. Protons and ^{3}He particles can be accelerated at energies higher than the meson threshold. Expected beam intensities at the target are 1 pμA for these ions and several tens of pμA for light and very heavy ions, respectively.

Figure 1 presents a customary energy per nucleon vs. mass number diagram for the present SSC together with the major facilities now under construction in the world. Although the maximum energies of the SSC are strongly dependent on the performance of the heavy-ion source of the linac, we used the average charge number from the conventional ion source. Energy variability will be realized down to 10 MeV/u for most kinds of ions.

2. General description of the accelerator complex.- As described above, the accelerator complex consists of the K=540 SSC and two injectors, one being the heavy ion linac and the other a K=90 AVF cyclotron. The linac and cyclotron can be used as an independent accelerator.

Examples of operating parameters at maximum energies are listed in table 1 for several kinds of ions. The beam from the injectors will be injected into the SSC after passing through a charge-stripping foil. The SSC can accelerate ions with different charge states with corresponding magnetic fields. In table 1, the optimum charge states are listed for the SSC.

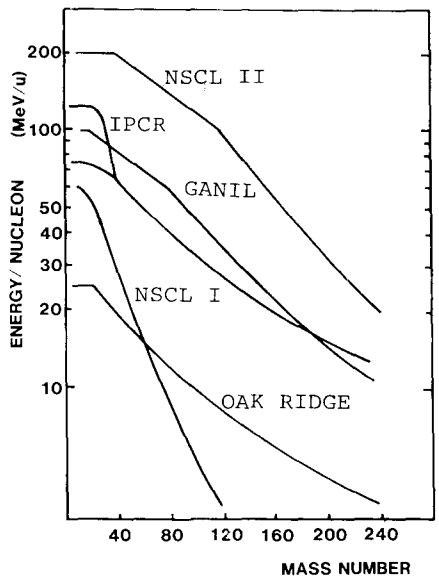

Fig. 1 : Maximum beam energy vs. mass number of the IPCR SSC together with those of heavy-ion accelerators in operation or under construction in some other laboratories.

The relation between the frequency and energy per nucleon in the linac is shown in figure 2 for different values of m/q on which the maximum energy of ions depends strongly. So it is possible to increase the maximum energy by developing the high charge ion sources for ions heavier than ^{40}Ar.

Coupling condition of the beam between the linac and the SSC gives the following restrictions: Path length of the first equilibrium orbit of the SSC should be equal to the integral multiple of the length of the last drift tube of the linac, and the frequency of accelerating voltage should be exactly the same for both accelerators. The linac accelerates ions over a frequency range from 17 to 45 MHz. Considering the coupling condition and the maximum field strength of

the sector magnet, the harmonic number h of the SSC was determined to be 9. Then the injection mean radius is fixed to 0.89 m. These values are different from those reported previously[1]. The reason why the parameters were changed is to reduce the maximum field strength and to keep a wider space in the central region of the SSC. The maximum value of B_{inj} was reduced from 1.7 T to 1.55 T and the injection mean radius was increased from 0.79 to 0.89 m .

The coupling condition between the SSC and the injector cyclotron has to be taken into account, too. The simplest combination of the parameters is obtained when the extraction radius of the injector cyclotron is equal to the injection mean radius of the SSC and also the ratio of the harmonic number of both accelerators is an integer. Since the injector cyclotron will be operated in the orbit frequency range of 2.7 to 7.5 MHz, h=3 and 6 are chosen as favourable values for the injector and the SSC, respectively. Figure 3 shows the relation between the orbit frequency and the energy per nucleon for acceleration with different harmonic numbers.

Table 1: Examples of operating parameters at the maximum energies in the present accelerator complex

	Ion	^{40}Ar	^{84}Kr	^{132}Xe	^{238}U
Linac	Charge q_1	8+	9+	9+	10+
	m/q_1	5	9	15	24
	$F_{Acc.}$(MHz)	43.3	33	26	20.4
	E(MeV/u)	3.8	2.2	1.36	0.84
SSC	Charge q_2	15+	24+	30+	37+
	m/q_2	2.7	3.5	4.4	6.4
	B_{inj}(T)	1.45	1.45	1.43	1.64
	B_{ext}(T)	1.55	1.5	1.46	1.66
	$F_{orb.}$(MHz)	4.8	3.67	2.88	2.27
	$F_{Acc.}$(MHz)	43.3	33.0	26.0	20.4
	h	9	9	9	9
	E(MeV/u)	66.6	36.8	22.3	13.6
	Ion	$p(H_2)$	^{3}He	^{12}C	
Cyclotron	Charge q_1	1+	2+	4+	
	m/q_1	2	1.5	3	
	$F_{Orb.}$(MHz)	7.37	7.37	6.51	
	F_{RF}(MHz)	22.1	22.1	19.6	
	B_{ext}(T)	0.97	0.727	1.28	
	E(MeV.u)	9	9	7	
SSC	Charge q_2	1+	2+	6+	
	m/q_2	1	1.5	2	
	B_{inj}(T)	0.833	1.26	1.48	
	B_{ext}(T)	0.994	1.49	1.67	
	$F_{orb.}$(MHz)	7.37	7.37	6.5	
	$F_{Acc.}$(MHz)	44.2	44.2	39.1	
	h	6	6	6	
	E(MeV/u)	184	184	134.6	

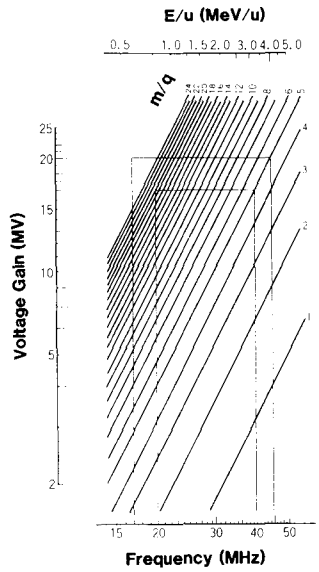

Fig. 2: Relation between frequency and beam energy of the injector linac.

The beam lines of the linac and the SSC are not in the same horizontal plane and the difference of the beam levels between two machines is about 12 m. Then the beam from the linac should be transported vertically by the above length as well as horizontally by about 40 m. We decided to adopt a canted injection method, i.e. the injection along a trajectory sloping to the median plane by 45° into the central region of the SSC. In the present case, the canted injection has an advantage over the radial injection, because the stray field in the open space between two sector magnets is not small at high magnetic field so that

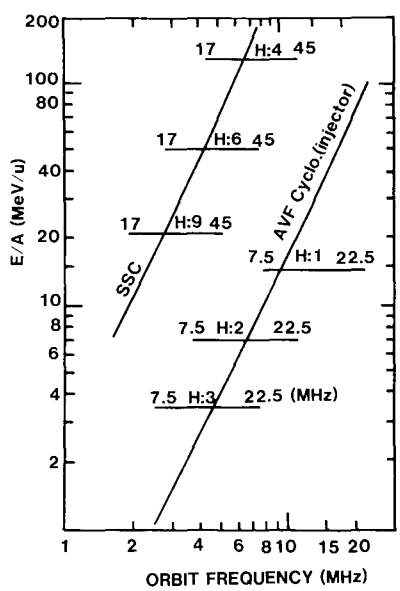

Fig. 3 : Relation between orbit frequency and beam energy of the SSC and the injector cyclotron for acceleration with different harmonic numbers.

the injection trajectory moves considerably depending on the ions and their energies. By putting quadrupole magnets along the canted trajectory between two vertical bending magnets, achromatic beam transport in the vertical direction can be realized.

The beam transport system between the injectors and the SSC are designed to guide the beam efficiently to the injection point in the SSC and also to match the beam quality with the acceptance of the SSC at that point. The beam ellipses in the transverse and longitudinal phase spaces should be well matched with the eigen ellipses of the first equilibrium orbit in the SSC. RF bunchers will be installed to get the RF phase focus at the injection point, too.

Ions from the injector is guided onto the acceleration orbit through a bending magnet, two magnetic inflection channels and an electrostatic inflector. The injection condition for the beam onto the well-centered orbit is obtained analytically and substantiated by numerical calculations.

Ions are accelerated by two delta-shaped electrodes installed in the opposite valley spaces between the sector magnets. To make certain of changing the frequency of the resonating cavity of the RF system over a range of 17 to 45 MHz, a half wave-length coaxial resonator with a shorting panel is adopted. RF electric field distributions along the accelerating gaps and the quality factors were measured for several types of half-scaled model cavities. Effective accelerating voltage will be 250 kV for the linac-injected ions whereas 170 kV for the cyclotron-injected ions.

Detailed design of vacuum chamber, RF resonator cavities and injection and extraction elements is now in progress.

3. Variable-frequency linac[2].- The principle of the variable-frequency linac is described by the following relation;

$$L = k \frac{1}{f}\sqrt{\frac{T}{m}} = k \frac{1}{f}\sqrt{\frac{q}{m}\Sigma V},$$

where L is length of the unit cell of the drift tube, f is the frequency of the linac, T is the energy of ions, and ΣV is the sum of effective accelerating voltage. Usually L is a fixed value, and if f is also fixed, ΣV must be changed proportionally to m/q in order to maintain the synchronized acceleration for ions having the different m/q values. On the otherhand, if the frequency can be changed so that light ions are accelerated with higher frequency and heavy ions with lower frequency, we can easily accelerate light ions up to higher energy than the heavy ions. Because of this characteristic, the variable-frequency linac is more suitable for the injector of the cyclotron than the fixed frequency linac.

A schematic drawing of the RF resonator is shown in figure 4. The resonating frequency can be changed by moving the shorting panel up and down. The linac has six cavities of the same shape and total voltage gain is expected to be 20 MV at maximum. The relation between the voltage gain and the frequency (or energy per nucleon) are shown in figure 2.

4. Calculation of the beam dynamics[3),4)].- Several computer codes for the orbit calculation have been developed and the orbit analysis has been extensively

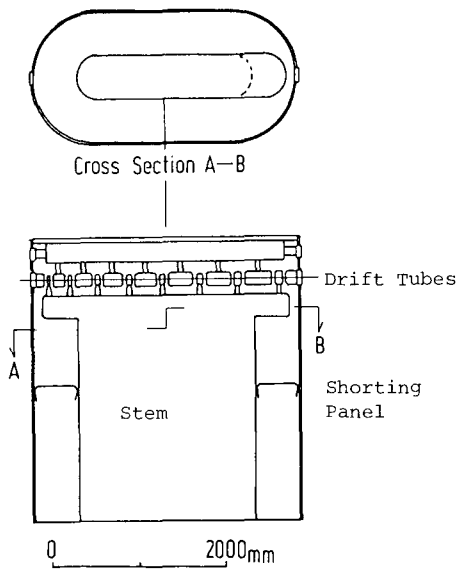

Fig. 4 : Schematic drawing of the RF resonator of the linac.

carried out. Magnetic field distributions used in these calculations were obtained from those measured for the 1/4 scale model of the sector magnet. A computer program named EQUIOT was used to form the isochronous field and to find the equilibrium orbits for several kinds of ions at various injection energies. The main characteristics of the SSC can be studied by calculating betatron frequencies, eigen-ellipses, phase plots and so forth.

Betatron frequencies in ν_z-ν_r space are given in figure 5 for typical particles of U^{40+} with the injection energy of 0.84 MeV/u, C^{6+} of 4 MeV/u and 7 MeV/u, and protons of 9 MeV. As can be seen in the figure, the 9 MeV proton beam crosses two resonance lines; $\nu_r - 2\nu_z = 0$ (Walkinshaw resonance) and $3\nu_r = 4$. The former is a quadratic, non-linear coupling resonance and the latter is quadratic, non-linear intrinsic resonance for the SSC composed of four sector magnets. The proton beam encounters these resonances at energies of nearly 128 and 165 MeV, respectively. The Walkinshaw resonance will generate an axial oscillation amplitude twice as large as any existing radial oscillation amplitude. Careful calculation of the radial and axial half widths of the beam before and after the resonances confirmed that they give only a slight change in the beam width.

Dynamics of the accelerated beam was calculated by the computer code ACCELP. The isochronous field distribution, geometrical shape of accelerating electrodes and radial- and frequency-dependence of the voltage distribution should be given in advance of the calculations. The isochronous fields were obtained from the calculation by EQUIOT whereas the voltage distribution along the accelerating gap was assumed to be constant, typically of 250 kV. The ray tracing calculations were performed simultaneously for 10 particles, one is the reference particle and the others are auxiliary particles with different initial values of parameters in the six-dimensional phase

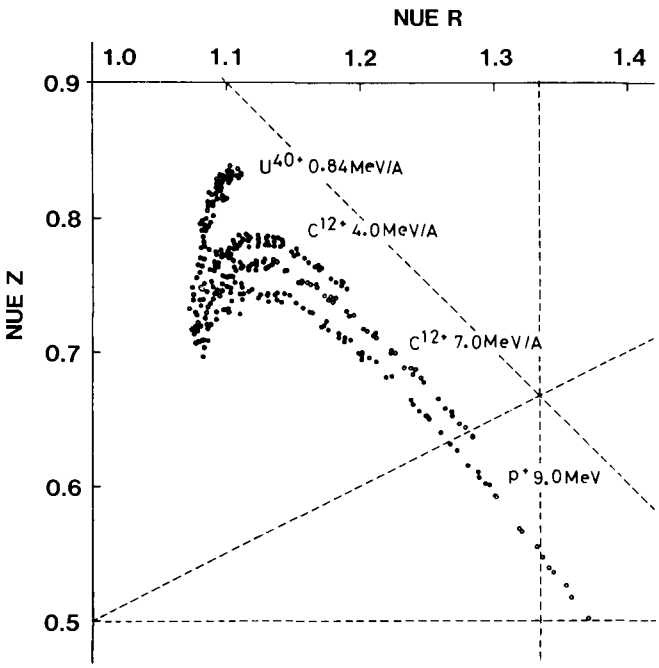

Fig. 5 : Betatron frequencies for typical ions.

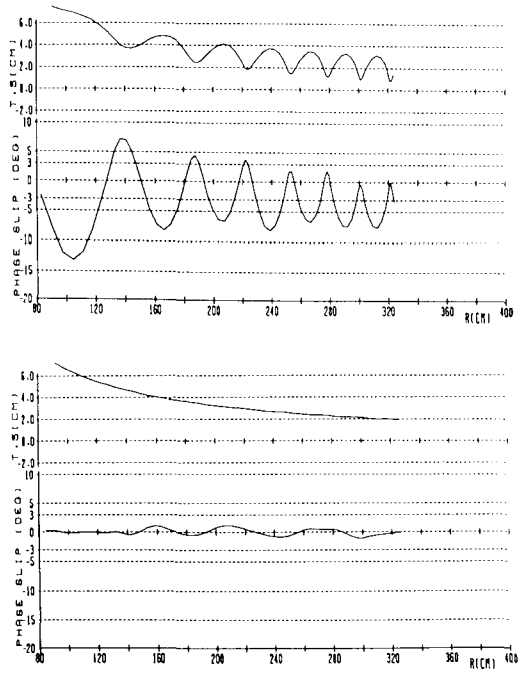

Fig. 6 : Turn separation and phase slip vs. radius for 0.84 MeV/u U^{40+} ions. The upper and lower figures correspond to the cases of off-centered and well-centered beams, respectively.

space with respect to the reference particle.

The condition for the acceleration in the well-centered orbit is that the beam should be injected onto the equilibrium orbit with a radial gradient (r') of proper value and also with an appropriate phase shift (ϕ_o) to the RF voltage so that the coherent radial oscillation amplitude is minimized. This condition also gives the minimum phase slip of an accelerated ion against the RF voltage. Figure 6 shows the results of the calculation of the turn separation and the phase slip at an azimuthal angle of 90° as a function of r. Upper and lower figures correspond to the cases of r' = 0, $\phi_o = 0$ (off-centered orbit) and r' = 31.78 mrad, $\phi_o = -14.0^\circ$, respectively.

The quality of the accelerated beam was evaluated by ray tracing calculation. The matching of phase parameters at the injection point plays an important role. For example, the matching conditions as $\Delta\phi_o = -hr' \times (R_{in}/\bar{R})$ and $r = R_{in} \times (dE/2E)$ are specially significant. Here h, R_{in} and $\bar{R}$ are the harmonic number, the injection radius and the mean radius of the first equilibrium orbit, respectively.

Another example is shown in figure 7 where the transformation of beam properties (radial emittance, radial half width, full phase width and energy resolution) is illustrated as a function of r for the central particle and four other particles.

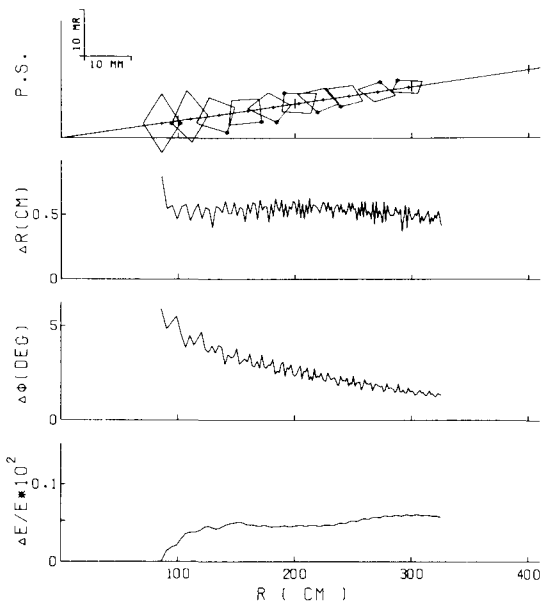

Fig. 7 : Transformation of beam properties (radial emittance, radial half width, full phase width and energy resolution) calculated at the mid-line of open valley.

In order to bring the injected beam onto the well-centered orbit, harmonic field will be applied on the base field. The behavior of the beam in the presence of the first harmonic field was studied by using the computer code INJHARM. In the calculation a off-centered beam was artificially given by putting the beam onto the equilibrium orbit at the injection point. Figure 8 shows the motion of the orbit center as a function of the turn number together with the direction and strength of the harmonic field(an arrow).

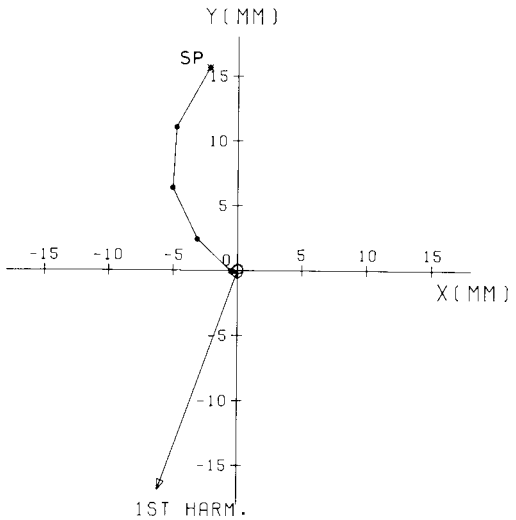

Fig. 8 : Motion of the orbit center for centering of 0.84 MeV/u $^{238}U^{40+}$ beam. The strength and angle of the first harmonic field are 24 Gauss and 250°, respectively. The exit of EIC is positioned in the direction of x axis. SP stands for the starting point of the orbit center.

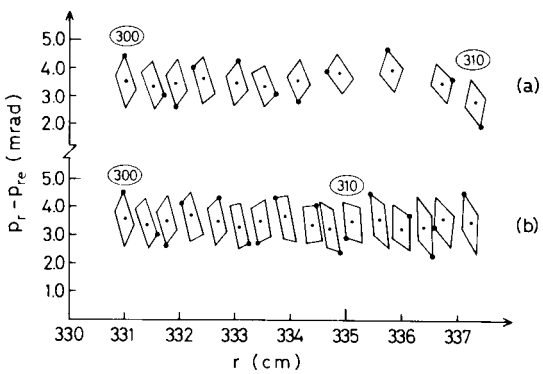

Fig. 9 : Radial phase space envelopes for 134 MeV/u $^{12}C^{6+}$ beam near extraction; a) with and b) without the first harmonic field. The numbers refer to the revolutions of the beam. Beam emittance is taken to be 20 mm·mrad.

Calculations of the beam trajectories through the injection and extraction elements were performed using the program codes, INJECT and EXTRACT, respectively. Another code, EXTHARM, was developed to calculate the effect of the harmonic field on the beam separation at the extraction radius. The turn separation of low energy light ions and heavy ions due to acceleration is large enough for single turn extraction in the SSC. However, this separation is not enough for high energy light ions so that the first harmonic field will be required to enlarge the beam separation. Furthermore we aim to extract the beam before $\nu_r = 1$ resonance to avoid the degradation of the beam emittance. Figure 9 shows the phase space envelopes of the beam around the extraction radius with and without the harmonic field. It can be seen that the beams are well separated at the extraction point. The degradation of the beam emittance cannot be seen at all during this process.

5. Sector magnet[5].- The plan of the SSC is shown in figure 10. The SSC consists of four sector magnets, two RF resonator cavities, the vacuum chamber which can be separated into eight chambers, injection and extraction elements, beam diagnostic devices and so on.

The sector magnet will produce the magnetic field in the range of .7 T to 1.55 T. The profile of the field distribution should provide the isochronism, focusing property and orbital stability for the beam in a wide range of energies and particles. After field measurements on the 1/4 scale model magnets and many calculations on the beam dynamics based on the above measurements, the final parameters of the sector magnets were determined as follows: the magnet has a sector angle of 50° and a gap of 8 cm. The maximum magnetomotive force was estimated to be 1.35×10^5 A.T. and the maximum power consumption in the four sector magnets is estimated to be 480 kW. The shape and geometrical size of the sector magnet are shown in figure 11. Extremely tight tolerances are required for stability of magnetic field, accuracy of machining and alignment of the magnets.

The pole edge profile is approximated by B-constant one except for the inner part where the side of the pole is cut away to keep a wider space for the RF resonators. Fringing field produced by this pole edge was investigated by comparing the results of calculations with TRIM code and the measured field of the model magnet. The difference of the field boundary between them was small and effective sector angle was found to agree with the designed value of 50° within 0.5°. Very homogeneously forged steel with carbon contents less than 0.02 % was used for the pole.

The yoke is to be divided into 16 slabs for the convenience of the construction and transportation. The ratio of cross-sectional area of yoke to that of the pole base is 0.94. Rolled steel with carbon contents of 0.08 % will be used for the yoke. Mechanical deformation of the yoke and poles due to the strong magnetic force, gravitational force and atmospherical pressure was calculated by a computer code FEM-2. The maximum deformation of 0.13 mm and vertical displacement of 0.35 mm were obtained. Putting a Purcell's gap between the yoke and the pole, we could reduce the deformation to 0.1 mm. Another calculations for the mechanical deformation have been carried out by using SAP-5[6] code and gave the same results.

For forming the required isochronous field, twenty-nine pairs of trimming coils are mounted on the pole face. Five pairs of them are also used for the harmonic field formation. They have curved shapes

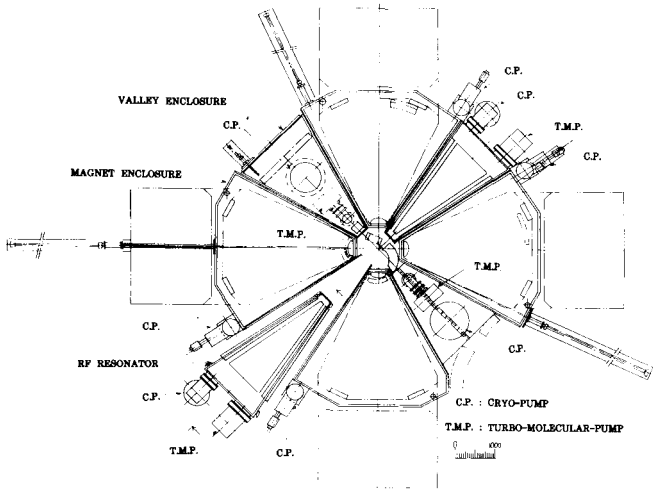

Fig. 10 : Plan view of the separated sector cyclotron

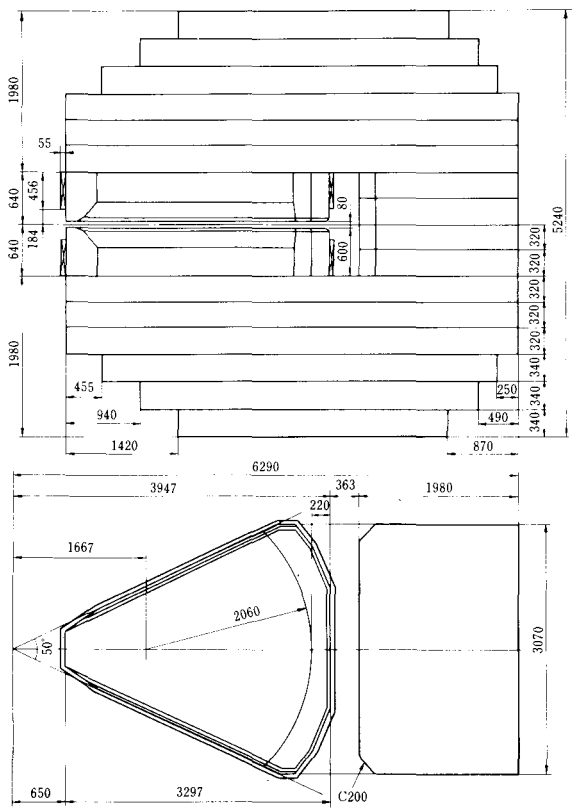

Fig. 11 : Shape and geometrical size of the sector magnet.

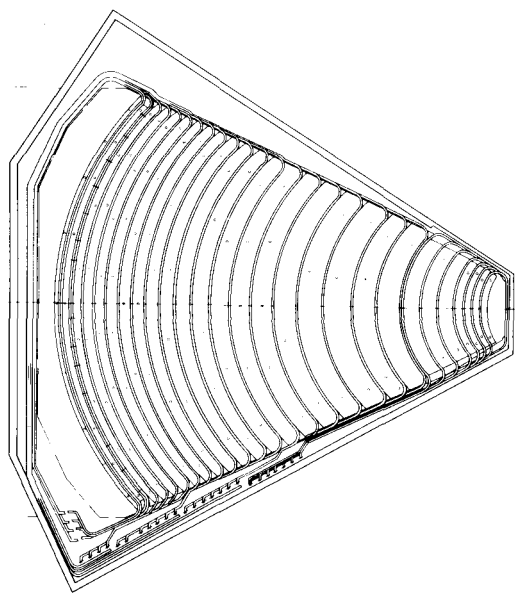

Fig. 12 : Lay-out of the trim coils for the sector magnet.

along the hard-edge equilibrium orbit (Gordon trajectory). The lay-out of configuration of the trim coils is shown in figure 12.

The radial width and position of each trim coil was determined from the optimization of the trim coil configuration. Difference between field distribution formed with 29 trim coils and a theoretical isochronous field is oscillating as a function of r with maximum amplitude of less than 0.1 %.

The effect of the discrepancy between the ideal and the practical isochronous field distributions of the beam quality was investigated by the calculations of the beam dynamics in which a perturbed field periodically varying along the radial direction was taken into account. The results show that the trim coils wound along the Gordon trajectory give better energy resolution if the perturbed field is rapidly varying with r.

Trim coils will be fixed directly on the pole face. In order to reduce the field perturbation due to bolt holes as low as possible, special bolts of soft iron welded onto stainless steel will be used.

The sector magnets as well as power suppliers were ordered to Sumitomo Heavy Industry Co. Ltd. The first one will be completed at the end of next March.

6. RF system[7]. - The RF system is required to satisfy the following conditions; the frequency range is 17 MHz to 45 MHz for the synchronous operation with the injector linac, the energy gain per turn per unit charge is 1 MeV, radial length of the accelerating gap should be longer than 2.65 m corresponding to the injection and extraction radii of 0.81 and 3.26 m at valley, respectively. The voltage distribution along the acceleration gap should be flat or radially increasing. Two resonators will be installed in the opposite valley spaces between sector magnets. In order to fulfil the above conditions, three types of the resonators were investigated, that is, a single gap type, a $\lambda/4$ type with single vertical stem and a $\lambda/2$ type with two vertical stems in the opposite sides. Although the first one has an advantage of simple structure and high Q-value, spatial restriction in the central region of our SSC makes the voltage at the dee gap low near the injection orbit. Moreover voltage twice as high is needed to keep the same energy gain per turn as compared with other types.

As for the second one, it was found from model study that a large RF electric field exists even inside of the dee. Therefore, we have to employ the third one and extensive studies have been done for half scale model resonator. Calculations based on the distributed parameter theory showed that stems having a cross sectional shape of race track have a good characteristic. Then a half scale model was made to investigate RF characteristics. Resonance frequencies, quality factors and voltage distributions were measured.

Figure 13 shows a schematic drawing of the resonator cavity which is now under investigation. It has 20° delta shaped dees. Moving short are used to change frequency and moving panels are also used at low frequencies. By using the moving panels in the low frequency region, we could improve the voltage distribution at large radii as shown in figure 14, and also could shorten the total length of the resonator. The structual analysis using the finite element method (SAP-5) is now in progress.

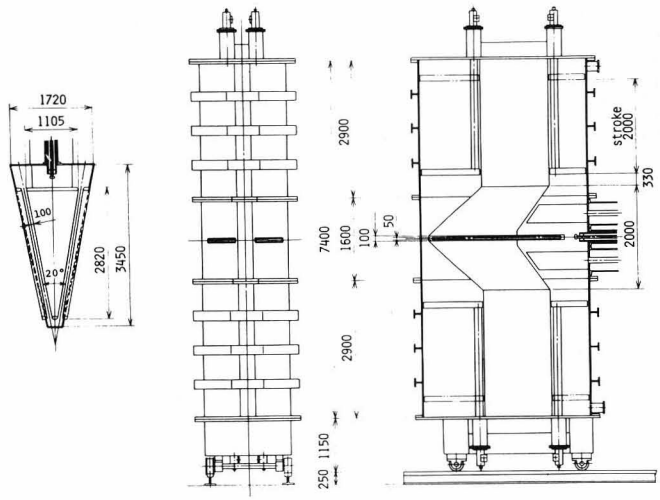

Fig. 13 : Schematic drawing of half wave resonator.

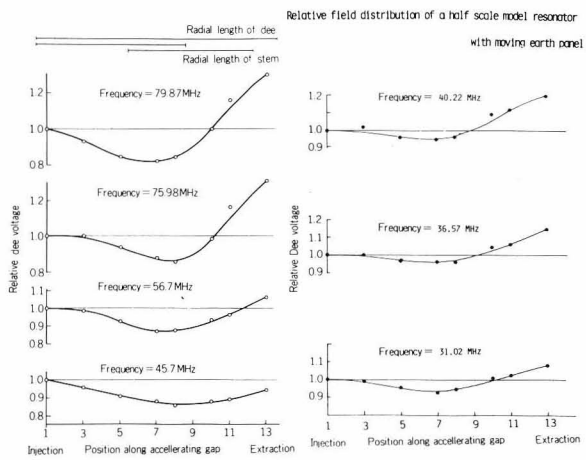

Fig. 14: Relative distribution of RF electric field along the dee edge of half scale model resonator. (a) without moving panel (b) with moving panel Measurements were done by perturbation method using ceramic block.

This type has some disadvantages as follows; the vertical length is long, maximum current density at sliding short fingers amounts 70 A/cm at 45 MHz for a voltage of 250 kV, and many undesirable resonances appears. Therefore, in parallel with this resonator, new method to vary the frequency is under investigation.

MOPA (master oscillator and power amplifier) system will be employed for a RF oscillator system. Synchronous operation with the injectors is necessary in a wide range of frequency. Because the maximum voltage at the accelerating gap should be 250 kV, maximum output power is to be 300 kW. An RCA 4648 tetrode will be used for the final power amplifier. Details of the power amplifier system and coupling system are now under investigation.

7. Beam injection and extraction system[8),9)].- The injection system has a principal role to guide a beam from the injector onto the first accelerated orbit in the SSC. The layout of the injection lines between the linac and the SSC and between the cyclotron and SSC is shown in figure 15. As mentioned in section 2, levels of the beam lines in the linac and in the SSC are different so that the beam from the linac should be transported vertically as well as horizontally to the SSC. We adopted the canted injection, that is, the beam is transported along the canted line in the vertical plane onto the median plane of the SSC. Passing through the bending magnet (BM1), two magnetic inflection channels (MIC2 and MIC1) and the electric inflection channel (EIC) the beam will be guided onto the acceleration orbit of the SSC at the exit of EIC. The layout of these injection elements together with the extraction elements is shown in figure 16.

The beam transport line between the linac and the SSC is composed of two types of subsystems, one is an achromatic beam bending section and the other is a straight beam guiding section with several quadrupole magnets. A charge stripping device is placed at SL0 which is the starting point of the transport system. The vertical section between SL0 and SL3 in figure 15 can play a role of not only an achromatic transport system but also an momentum analyzer system. A beam buncher will be installed at SL3 and make a waist in l-δ space at the beam injection point in the SSC. The section between SL3 and SL4 converts the shape of the beam ellipse so as not to diverge in the subsequent sections. The complete dispersion matching is carried out by using the section between SL4 and SL5 together with the injection system in the SSC. The transverse phase space matching is realized by four quadrupole magnets between SL5 and SL6. The second order calculations are also carried out to estimate the beam aberrations which are found to be very small.

The beam from the injector cyclotron is made to form a double-waist at SC0 by a quadrupole triplet. Hereafter SC0 is the starting point of the beam transport line between the cyclotron and the SSC. The section between SC0 and SC2 transform the dispersive beam into the achromatic one. The section between SC2 and SL5 composes an achromatic transport line with 90° bend.

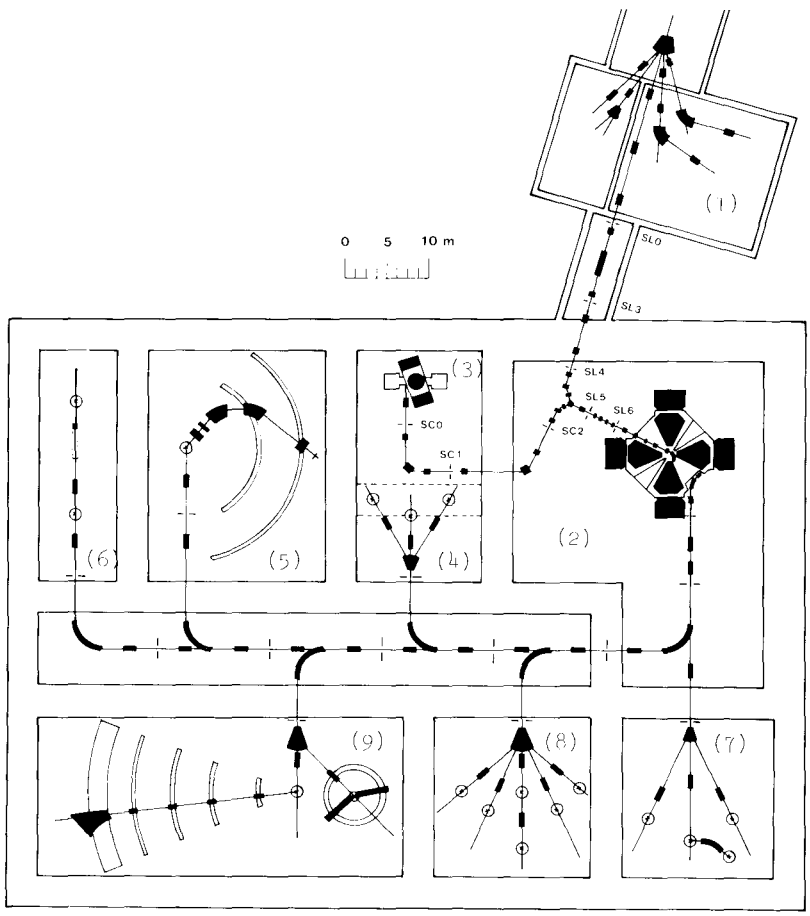

1) Experimental hall for linac
2) SSC vault
3) AVF Cyclotron vault
4) Material irradiation
5) Nuclear Physics
6) Radio therapy
7) RI production
8) Atomic Physics
9) Nuclear Physics

Fig. 15 : The plan view of the beam transport system for the IPCR SSC. The beam levels of the SSC, the linac and the AVF cyclotron are not on the same horizontal plane.

The canted injection line starts from SL6. The advantage of this type of the injection is already mentioned. We could put the beam focusing and steering elements down to the central region of the SSC. In order to realize the acceleration in the well-centered orbit, not only the position and direction but also the dispersion in radial direction and the beam ellipse in six dimensional phase space should be well matched at the injection point. In the present SSC the matching will be accomplished by adjusting these injection elements.

The design works of the injection elements are now in progress. Excitation curve and field distributions were measured for the model bending magnet. The field distribution of the magnetic inflection channel was also studied by the model MIC.

Extraction elements are also shown in figure 16.

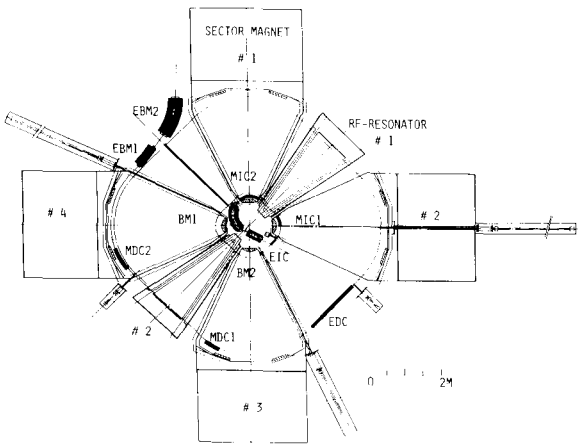

Fig. 16 : Layout of beam injection and extraction elements of the SSC

Low energy light ion and heavy ions can be extracted by acceleration. On the other hand, the high energy light ions can be extracted by applying the first harmonic field and enlarging the turn separation of the beam. The beam will be peeled off by an electrostatic deflection channel (EDC) from the last acceleration orbit and guided out of the SSC by means of two magnetic deflection channels (MDC1 and MDC2) and two bending magnets (EBM1 and EBM2).

8. Vacuum system and chamber[10].- The SSC will accelerate not only light ions but also very heavy ions. The pressure in the chamber should be sufficiently low to reduce the beam loss due to the collisions with residual gas molecules. Operating pressure less than 1×10^{-7} Torr is desirable in order to keep the beam loss less than 10 % even for the very heavy ions. Schematic drawing of the chamber and the vacuum system is shown in figure 10. As can be seen in the figure, the chamber is divided into eight sections, two RF resonators, four magnet chambers and two valley chambers. In order to reduce outgassing from large surface area of poles, trim coils and insulating materials used with the trim coils as lower as possible, auxiliary vacuum chamber will enclose them and separate them from the high vacuum section of the main chamber. The main coils for the sector magnets are in the atmosphere. The spaces betwen sections are too narrow that the usual sealing methods for high vacuum is difficult to be employed. Pneumatic expansion seals seem to be much more practical and models were made for the operational test.

Total volume of the chamber is estimated to be 65 m^3 and the inner surface areas of principal materials are as follows; 300 m^2 of stainless steel, 440 m^2 of copper and 5 m^2 of elastomer. Total outgassing rate is estimated to be 8×10^{-3} Torr·l/sec after 20 hours pumping. Additional gas load from the leakage and surface of components installed in the chamber will be about 3×10^{-3} Torr·l/sec. Therefore the effective pumping speed of 11×10^{4} l/sec is necessary to keep the chamber under the required pressure. Turbo-moleculer pumps and crypumps will be installed as shown in figure 10.

9. Experimental halls and beam transport system[9].- This facility will be devoted to researches in various fields such as nuclear and atomic physics, solid state physics, material engineering, radiation chemistry and biology. To use the SSC for radiotherapy is also being considered. Many experimental facilities for these researchers are being planned to be constructed at IPCR. The layout of the beam lines and main facilities together with a plan view of the SSC and the injector cyclotron is shown in figure 15.

The design of the beam transport system to the experimental areas is now in progress. The main feature of it is that the double-monochromater system with two 90° bending magnets is used. Ion-optical calculations starting from the eigen ellipses of the beam in the last equilibrium orbit of the SSC are undertaken.

Environmental radiation is the serious problem in Japan. It is required that design of the shieldings should be aimed to keep the radiation dose due to the SSC as low as 5 mrem/year at the border of the campus. In order to realize this very low level at the border, thick concrete walls and ceilings as well as thick local shieldings will be adopted. In the present design of the building the thickness of the concrete walls and ceilings of the SSC vault should be 4 m and that of the other rooms should be 3 m. The shielding effect, sky shine and streaming of the high energy neutrons and the radiation doses at various points both inside and outside of the building are calculated[11].

10. Time schedule.- The first sector magnet will be completed at the end of nex March. Then the second one will be in June and the field measurement will be done for these two magnets. The cyclotron vaults will be build in 1983 and the complete field mapping will be done after that time. If everything will go well, we expect that we can ge the first beam at the middle of 1986.

References.

1. H. Kamitsubo et al., "A proposed multi-purpose separated-sector cyclotron at IPCR", Proc. of 8th Int. Conf. on Cyclotrons, Indiana, (1978) 2070.

2. M. Odera et al., "Status of the variable frequency heavy ion linac, RILAC", Proc. of 1979 Linear Accel. Conf., Montak, (1979) 28.
3. N. Nakanishi et al., "Beam dynamics for the IPCR SSC", This conference.
4. A. Goto et al., "Calculation of injection and extraction orbits for the IPCR SSC", This conference.
5. S. Motonaga et al., "The sector magnet for the IPCR SSC", This conference.
6. K.J. Bathe, E.L. Wilson and F.E. Peterson, "SAPIV- A Structural Analysis Program for Static and Dynamic Responce of Linear Systems", Report EERC 73-11, College of Engineering, University of California, Berkeley, June 1973, revised Apr. 1974.
7. M. Hara et al., "The RF system for the IPCR SSC", This conference.
8. Y. Yano et al. "Beam injection and extraction system for the IPCR SSC", This conference.
9. N. Kishida et al. "Beam transport system for the IPCR SSC", This conference.
10. S. Nakajima et al. "The vacuum system of the IPCR SSC", This conference.
11. S. Fujita et al. "Status of neutron shielding for the IPCR SSC", This conference.

" DISCUSSION "

S. ADAM (remark) : The formula for the difference between RF-phase and CP-phase has to be corrected by including a factor of $1/\nu_r^2$ as can be seen in paper "New proofs for old facts in acceleration theory" (this conference) or in a paper by M. GORDON and F. MARTI to appear in NIM.

H. KAMITSUBO : Thank you for your comments. In our case, we investigate the behaviour of particles at the different points on the phase ellipse by numerical calculations. The analytical formula was used to select the initial values for numerical calculations.

F.G. RESMINI : Can you comment on the use of advanced ion sources in your accelerator system ? Do you have any plans to actually build either ECR or EBIS sources ?

H. KAMITSUBO : The maximum energy of ions from the linac depends on m/q value as shown in figure 2, so that, if we will use the advanced ion source and succeed to get larger values of m/q for ions heavier than ^{40}Ar, we can increase the maximum energy easily. The linac group at IPCR is discussing a plan to develop the ECR ion source.